Multi-wavelength laser active coherent combination*

Han Kai(韩 凯)†, Xu Xiao-Jun(许晓军), and Liu Ze-Jin(刘泽金)

College of Opto-electronic Science and Engineering, National University of Defense Technology, Changsha 410073, *China*

(Received 23 August 2011; revised manuscript received 8 November 2011)

A seed laser oscillating at different frequencies is proved to have the potential to mitigate the stimulated Brillouin scattering (SBS) effect in a fiber amplifier, which may increase the emission power of a coherent beam combination (CBC) system greatly. In this study, a basic mathematical model describing the multi-wavelength CBC is proposed on the fundamentals of CBC. A useful method for estimating the combination effect and analysing the feasibility and the validity of the multi-wavelength coherent combination is provided. In the numerical analysis, accordant results with four-wavelength four-channel CBC experiments are obtained. Through calculations of some examples with certain spectra, the unanticipated excellent combination effect with a few frequencies involved is explained, and the dependence of the combination effect on the variance of the amplifier chain length and the channel number is clarified.

Keywords: fiber laser, coherent beam combination, multi-wavelength laser, optical path difference

PACS: 42.25.kb, 42.62.–b, 42.55.Wd **DOI:** 10.1088/1674-1056/21/5/054205

1. Introduction

Coherent beam combination (CBC) of fiber lasers/amplifiers can increase the output laser power from a single gain medium while simultaneously maintaining a good beam quality, which is becoming an important research area for high energy laser technology.[1,2] The CBC of fiber lasers can be classified into two categories: passive phasing and the active phasing in a master oscillator power amplifier (MOPA) configuration.[2−7] Active CBC is generally considered to be capable of scaling a large number of beamlets.

In active CBC, the power density of the combined beam is enhanced owing to the interference effect. It is conventionally believed that the interference occurs only under the condition of single frequency, the same polarization, and a steady phase difference.[8] Therefore, a single-frequency seed laser is often considered to be indispensable for improving the spatial coherence property in active CBC.[9] Nevertheless, single-frequency radiation restricts the output power of the coherently combined fiber amplifier because of the low stimulated Brillouin scattering (SBS) threshold. A broadband seed laser oscillating at different frequencies is proved to have the potential to mitigate the SBS effect and heighten the power in a fiber amplifier. For instance, when the wavelength separation is twice the Brillouin shift, a two-fold increase in the total output power can be obtained.[10] Moreover, the scalability of the diffraction-limited fiber laser has been analyzed by Dawson *et al.*[11] Some effects, such as non-linear effects, thermal effects, and fiber damage, limit the output power of the broadband fiber laser to around 36 kW, while the output power of the narrowband fiber laser is merely at a level of no more than 2 kW.[11] It means that the multi-wavelength laser has the capability of greatly increasing the emission power.

The feasibility, the validity, and the corresponding control strategy of multi-wavelength CBC quite differ from those of single-wavelength CBC due to the difference in the coherent property of a seed laser. These issues are highly attractive and have been studied by some scholars considering the promising future of multi-wavelength CBC. Several multi-wavelength CBC experiments have been reported, in which excellent combination effects were obtained and its feasibility was demonstrated.[12−16] However, few theoretical explanations have been given.[17]

In the present article, a basic mathematical model is proposed. With this mathematical model, the multi-wavelength active CBC experiments in Refs. [15]

*Project supported by the Innovation Foundation for Postgraduates in the National University of Defense Technology, China (Grant No. S090701).

†Corresponding author. E-mail: hankai0071@nudt.edu.cn

© 2012 Chinese Physical Society and IOP Publishing Ltd

and [16] are analysed, and comparatively compatible results are obtained. Through the calculation of the CBC example in Ref. [12], the periodic relationship between the combination effect and the optical path difference is revealed, and the unanticipated nice CBC effect is explained. By the numerical investigation of CBC with different spectra at various fiber chain cutting precisions, the dependence of the combination effect on the amplifier chain length and the channel number is demonstrated. Finally, the control strategy suited for multi-wavelength CBC is discussed.

2. Mathematical model

Figure 1 is a schematic diagram of a typical multi-wavelength CBC system in the MOPA configuration with active phase controlling. The master oscillator provides the seed laser containing several frequencies denoted as ν_1, ν_2, ..., ν_N. Through a fiber splitter, the energy of the beam is equally distributed into the power amplification (PA) systems with a phase modulator (PM) array. The amplified laser beams are collimated and output together. The output is sampled and then focused into a detector with a pinhole in front. The size of the pinhole is a little smaller than the main lobe of the focused beam. By using the stochastic parallel gradient descent (SPGD) optimization algorithm, the control signal can be computed and fed back to the PM array.[18,19] The energy distribution can be optimized if the convergence process is fast enough to compensate the phase noise.

According to the classical interference theory, the amplitude summation is used for components of the same frequency, while the intensity summation is used for components of different frequencies.[8] In this way, the combination effect of active CBC can be calculated.

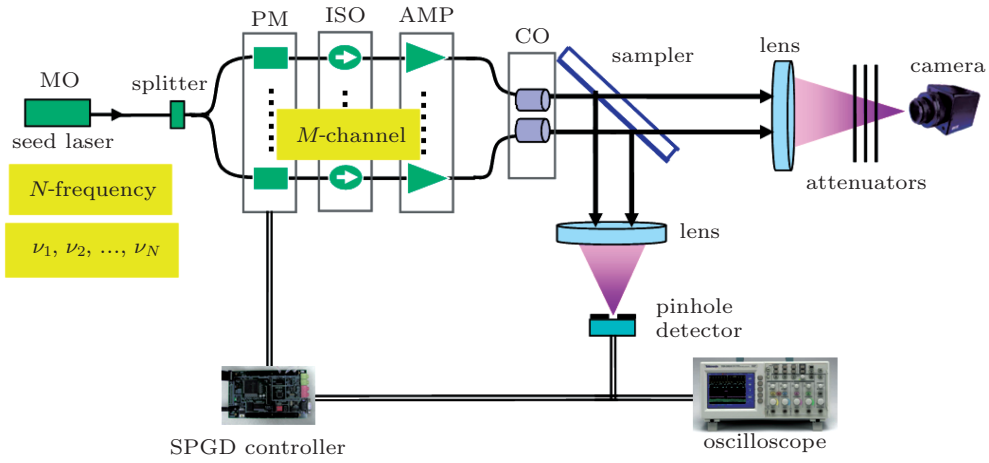


Fig. 1. (colour online) Schematic diagram of M-channel N-frequency multi-wavelength active MOPA configuration CBC.

In an M-channel N-frequency MOPA configuration CBC system (Fig. 1), each channel contains N frequencies, i.e., ν_1, ν_2, ..., ν_N. If the intervals of adjacent frequencies are equal, the interval can be denoted as $\mathrm{d}\nu$, and the width of the whole spectrum is represented by $D\nu$. There is an evident relationship among $D\nu$, $\mathrm{d}\nu$, and N, i.e.,

$$\mathrm{D}\nu = (N-1) \times \mathrm{d}\nu. \tag{1}$$

The n-th frequency can be written as

$$\nu_n = \nu_0 - (N-1)/2 \times \mathrm{d}\nu + (n-1) \times \mathrm{d}\nu, \tag{2}$$

where ν_0 is the central frequency of the spectrum. It is assumed that the beam in each channel is a Gaussian beam, then the complex-amplitude of ν_n-frequency in the m-th channel is given by

$$E_{m,\nu_n}(x,y) = \sqrt{a(\nu_n)} \cdot \omega_0/\omega_{\nu_n}(Z) \cdot \exp\left\{-\left[(x-x_m)^2 + (y-y_m)^2\right]/\omega_{\nu_n}^2(Z)\right\} \times \exp\left[-\mathrm{j}\left[2\pi \cdot \nu_n/c \cdot \left\{Z + l_m + \left[(x-x_m)^2 + (y-y_m)^2\right]/2R_{\nu_n}(Z)\right\} - \varphi_{0\,\nu_n} + \varphi'_{m,\nu_n}\right]\right], \tag{3}$$

where Z is the optical path in free space, l_m is the optical path in the m-th channel ($Z \gg l_m$), (x, y) are the coordinates in the observation plane, and (x_m, y_m) are the coordinates of the m-th channel beam center in the emission plane.

In this case, the complex-amplitude of the ν_j-frequency component in the combined beam is equal to the sum of the counterparts in each channel, which is written as

$$E_{\nu_n}(x, y) = \sum_{m=1}^{M} E_{m,\nu_n}(x, y). \tag{4}$$

The intensity of the ν_j-frequency component can be described as

$$I_{\nu_n}(x, y) = E_{\nu_n}(x, y) \times E^*_{\nu_n}(x, y). \tag{5}$$

The intensity of the combined beam is equal to the sum of the intensities at each frequency, which can be expressed as

$$I(x, y) = \sum_{n=1}^{N} I_{\nu_n}(x, y). \tag{6}$$

The intensity distribution of the combined beam in the M-channel N-frequency CBC system can be obtained according to formulas (1)–(6). The power in bucket (PIB), the beam propagation factor (BPF), and the contrast of the far-field intensity profile can be obtained from the intensity distribution of the combined beam. The BPF and the contrast are customarily used to evaluate the CBC effect.[12,20,21] The PIB is defined as the laser output power of the main lobe in the specified far field. The area of the main lobe is $A = \pi (1.22\lambda Z/D)^2$, where D is the effective exit aperture of the combined laser beam. Thus,

$$\mathrm{PIB} = \iint_A I(x, y)\, \mathrm{d}x \mathrm{d}y. \tag{7}$$

The BPF is given as the PIB multiplied by 1.19 and divided by the total laser output power radiated from the effective near-field exit aperture[20−22]

$$\begin{aligned} \mathrm{BPF} &= 1.19\mathrm{PIB}/P_{\mathrm{total}} \\ &= 1.19 \iint_A I(x, y)\, \mathrm{d}x \mathrm{d}y \Big/ \int_{-\infty}^{+\infty} \int_{-\infty}^{+\infty} I(x, y)\, \mathrm{d}x \mathrm{d}y. \end{aligned} \tag{8}$$

The contrast (CON) is defined as

$$\mathrm{CON} = (I_{\max} - I_{\min})/(I_{\max} + I_{\min}), \tag{9}$$

where $I_{\max}$ and $I_{\min}$ are the maximum intensity and the adjacent minimum intensity of the intensity distribution, respectively. The BPF is usually used to evaluate the combination effect when the channel number M is not very small, while the CON is suited for a few channels. The values of BPF and CON lie between 0 and 1, and the larger the two values are, the better the combination effect is.

3. Numerical calculation and analysis

3.1. Four-wavelength four-channel coherent beam combination

To clarify the reliability of the above-mentioned mathematical model, the multi-wavelength CBC experiment in Refs. [15] and [16] is investigated numerically. In Refs. [15] and [16], a four-wavelength four-channel ($N = 4$, $M = 4$) MOPA configuration active CBC experiment was conducted, the SPGD optimization algorithm was implemented, and a satisfactory result was obtained. The four wavelengths in Refs. [15] and [16] were 1060.7 nm, 1064.1 nm, 1064.5 nm, and 1083.2 nm, and the power at the four wavelengths was nearly the same. The spectrum is shown in Fig. 2. In the experiment, the cost function J increased from 25% of the ideal value in the open loop to nearly 75% of the ideal value in the close loop. The ideal PIB value was 0.284, and the PIB in the close loop was 0.235, which approached 82.7% of the ideal value. The intensity distribution of the profile indicated the contrast of the far-field interference pattern to be about 0.8.

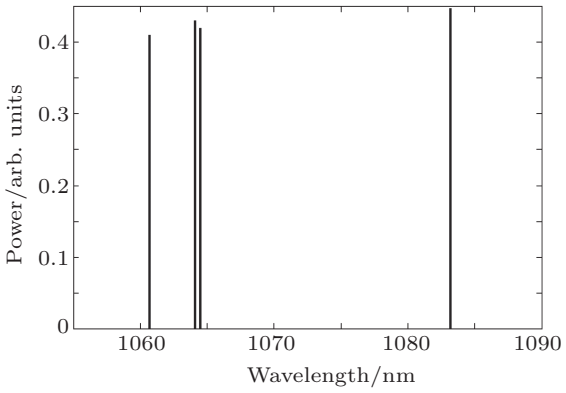


Fig. 2. Spectrum of four-wavelength four-channel CBC.

The configuration parameters and the control parameters in the SPGD algorithm are selected according to Refs. [15] and [16]. In Refs. [15] and [16], to

ensure the optical paths (l_m) of all channels to be the same, simple and rough measures were carried out by fiber cutting and fusion. Consequently, we assume that the variance of the optical paths (l_m) is around 1 mm in our calculation. The far-field intensity distribution is calculated according to formulas (3)–(6) and shown in Fig. 3. The contrast of the profile is found to be 0.779 with formula (9), which is a little smaller than the experimental result. The PIB is found to be 83.8% of the ideal value with formula (7). Based on formulas (3)–(8), the cost function J without and with active phasing can be calculated. Figure 4 shows the simulation result of 100 converging curves of cost function when the SPGD algorithm is performed with random initial phase noise. Due to various phase noises, the initial values of cost function J are different, of which the mean is 0.289. When the SPGD optimization algorithm is executed, the cost function J converges to 0.788. The calculated PIB and the cost function J are nearly as large as their experimental counterparts.

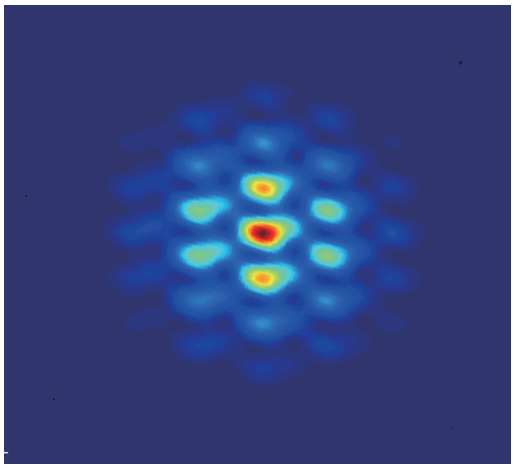


Fig. 3. (colour online) Far-field intensity distribution of four-wavelength four-channel CBC.

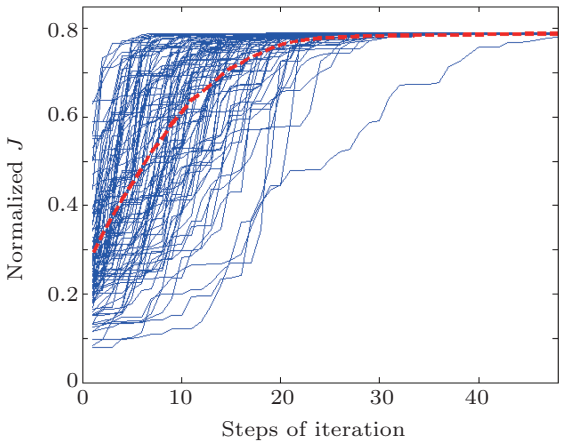


Fig. 4. (colour online) Converging curves of cost function J.

The above analysis shows that the calculated combination effect is consistent with the experiment in spite of some errors, and the model is competent to analyse the feasibility and the validity of multi-wavelength CBC and to estimate the multi-wavelength CBC effect.

3.2. Two-wavelength three-channel coherent beam combination

To clarify the feasibility of multi-wavelength CBC, the experiment in Ref. [12] is studied numerically. The experimental setup of CBC in Ref. [12] is composed of three two-tone fiber amplifiers, that is $N = 2$, $M = 3$. The two wavelengths are 1064 nm and 1083 nm, and the power of the two frequencies is the same. The spectrum is shown in Fig. 5. In the calculation, the configuration parameters are chosen according to Ref. [12]. The phase noise φ'_{m,ν_n} is introduced randomly. The original optical path differences Δl_{21} and Δl_{32} are defined as $l_2 - l_1$ and $l_3 - l_2$, respectively.

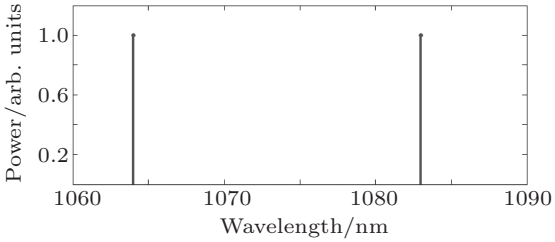


Fig. 5. Spectrum of two-wavelength three-channel CBC.

The far-field intensity distribution with certain optical path differences Δl_{21} and Δl_{32} can be obtained with formulas (1)–(6). The active phase control of each fiber channel is implemented with the SPGD algorithm according to the experiment in Ref. [12]. The control parameters accord with those of the experiment. The CBC effect is evaluated by the BPF and the CON, which are derived from formulas (8) and (9). The dependence of the combination effect on the optical path difference can be calculated, as shown in Figs. 6 and 7, where the unsmooth spots result from the SPGD algorithm limitation that the cost function cannot converge to the theoretical optimal value accurately every time.

The gray scales of the spots in Figs. 6 and 7 represent the normalized BPF and the CON, respectively. The periodic beating is the well known Talbot

re-images. With various original optical path differences, the BPF and the CON are both between 0.68 and 1. In other words, the system has lots of chances to achieve excellent combination effect even though the optical path differences are not zero. In the experiment of Ref. [12], the normalized BPF and the CON have reached 0.82 and 0.85, respectively. Under the condition that the optical path differences are chosen stochastically around 1 m, which is the same as that in the experiment of Ref. [12], the probability of the normalized BPF larger than 0.82 is 74%, and the probability of the CON larger than 0.85 is 86% based on our calculation result. This gives a preliminary explanation to the unanticipated excellent combination effect in the experiment. In a word, the two-wavelength laser has well coherent property in CBC despite of the large original optical path difference.

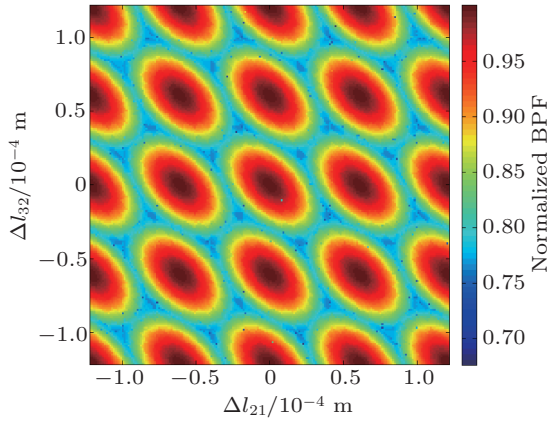


Fig. 6. (colour online) Dependence of BPF on optical path difference.

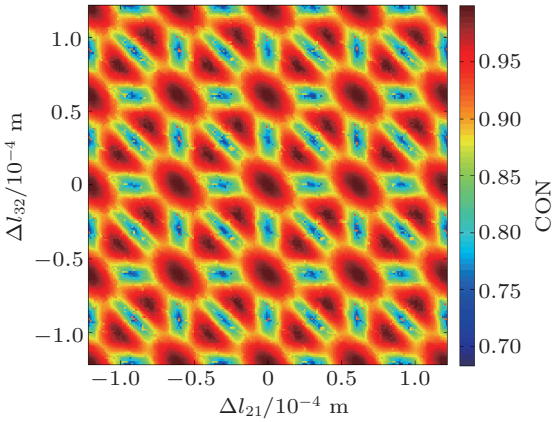


Fig. 7. (colour online) Dependence of contrast on optical path difference.

3.3. Dependence of combination effect on chain length variance

In a practical application, a common approach to obtain an excellent CBC effect is to make the original optical path difference be zero. However, it is difficult to make the lengths of all channels equal to each other accurately in practice.[23] Under the condition of endeavouring to make the amplifier chains have equal lengths, the optical paths of the channels usually obey a normal distribution with mean μ and standard deviation σ. The standard deviation σ depends on the technical level, which determines the multi-wavelength CBC effect. Consequently, it is necessary to investigate the dependence of the combination effect on the fiber chain cutting level in various configurations with the multi-wavelength seed laser involved.

The N-wavelength (N = 2, 4, 6, 8) M-channel (M = 7, 19, 37, 61) MOPA configuration CBCs are taken as examples. The spectra are shown in Fig. 8. In the calculation, the configuration parameters are selected according to Ref. [12]. The fill factor t is assumed to be 0.5, and $t = (d - 2w_0)/w_0$, where d is the distance between the nearest neighbors.[20,21] The

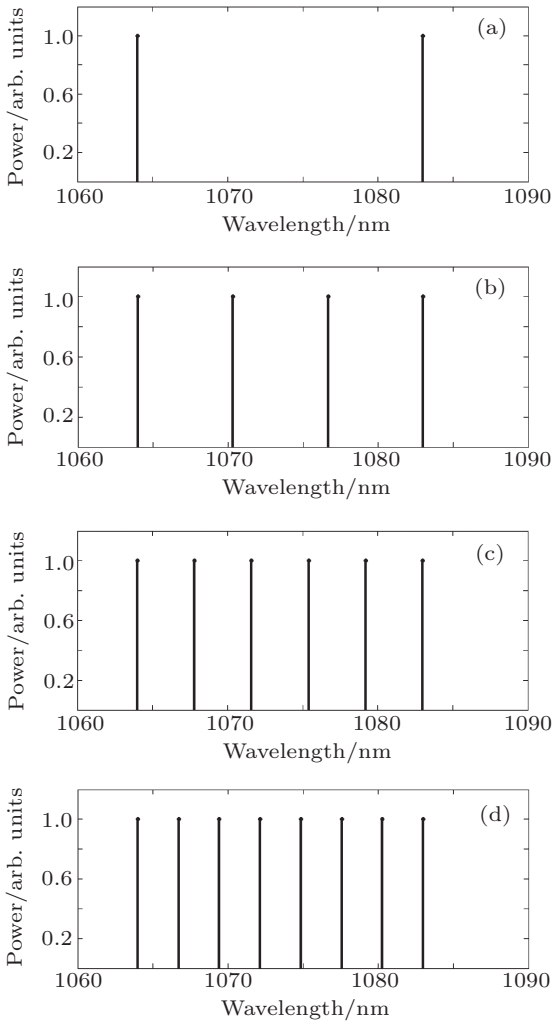


Fig. 8. Spectra of (a) 2-, (b) 4-, (c) 6-, and (d) 8-wavelength CBCs.

phase noise φ'_{m,ν_n} is also introduced randomly. The optical path in m-th channel l_m ($m = 1, 2, \ldots, M$) obeys a normal distribution with mean μ and standard deviation σ, that is $l_m \sim N(\mu, \sigma^2)$, $m = 1, 2, \ldots, M$. The SPGD algorithm is also implemented to lock the phases of the beams. The combination effect is also evaluated by the BPF according to formulas (1)–(8). Considering the randomicity of l_m ($m = 1, 2, \ldots, M$), we perform the calculation many times (2000), and the result is then averaged over them. The dependence of the BPF on fiber cutting precision level σ in N-wavelength M-channel CBC is shown in Fig. 9.

Figure 9 shows that the holistic combination effect becomes worse when more wavelengths are involved. The combination effects with a few wavelengths are passable at diverse optical path variances for various configurations. With the optical path variance increasing, the degenerating trends of the combination effect for different N become similar to each other. The BPF decreases as variance σ of the chain length increases, which is for all kinds of configurations. The normalized BPF decreases gently when σ is small, and plunges at $\sigma \sim 10^{-5}$ m, which accords with the coherent length of the spectrum. Finally, the BPF stabilizes at some levels. The combination effect in a large array is worse than that in a small array, while the distinction turns unnoticeable with the laser number increasing. In summary, in the few-wavelength CBC system, it is comparatively unnecessary to make the chain lengths equal, as the combination effects are fair for diverse variances of optical paths. However, to gain a desirable combination effect with several wavelengths, especially for large beam number arrays, the variance of the chain lengths should be adjusted to be smaller than the coherent length. In experiment, a common optical path control method is to hold the fiber cutting and fusion precision and to tune the optical path of each beam in the free space. To gain an excellent effect in a many-wavelength seeded CBC system, the whole spectrum should not be wider than 1 nm.

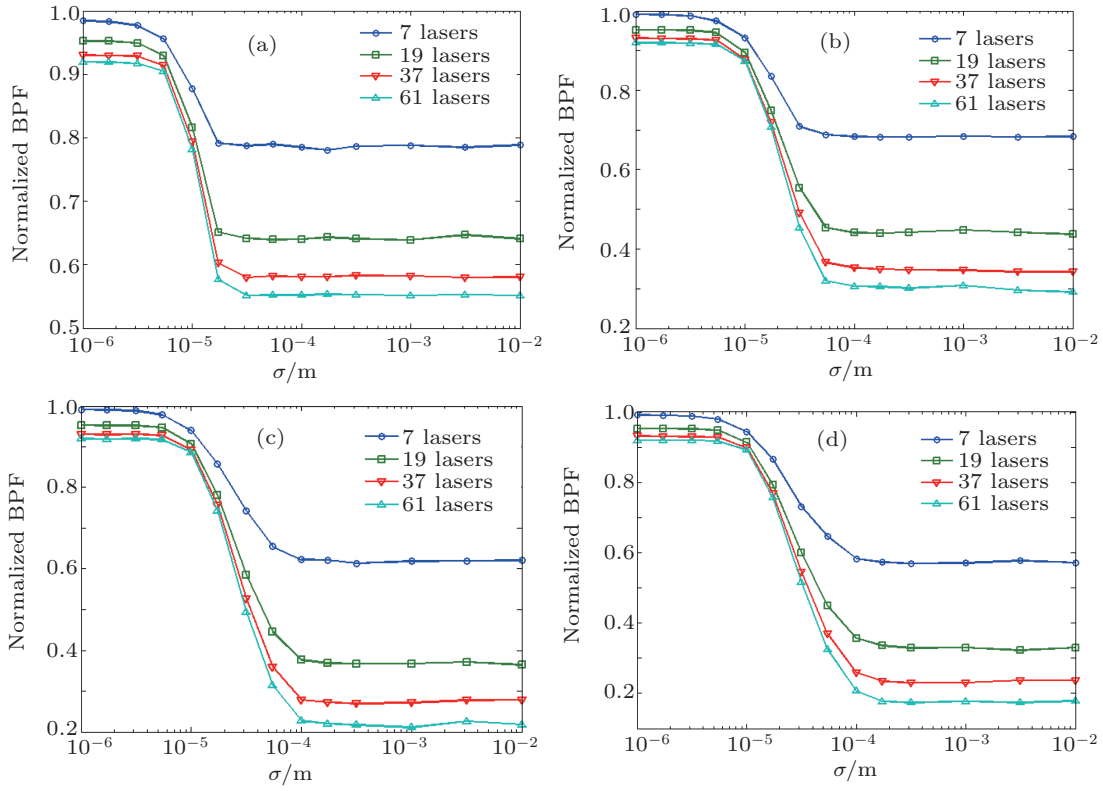


Fig. 9. (colour online) Dependences of BPF on σ for (a) 2-, (b) 4-, (c) 6-, and (d) 8-wavelength CBCs.

4. Conclusion and discussion

The multi-wavelength laser has the potential to increase the emission power due to its high SBS threshold. It is quite attractive to employ a multi-wavelength laser in CBC. A mathematical model is proposed on the principles of CBC. In the numerical analysis of the four-wavelength four-channel CBC

experiment in Refs. [15] and [16], accordant results are obtained. The model is competent to investigate multi-wavelength CBC theoretically. By using the model, the feasibility and the validity of multi-wavelength CBC are studied. In multi-wavelength CBC, the combination effect depends on the original optical path difference, and the relationship is periodic. With the optical path difference increasing, the combination effect does not always degrade but changes periodically. Apparently, when several wavelengths are involved, an effective approach to gain an excellent CBC effect is to accurately cut the fiber chains into the same length. The dependence of the combination effect employing N(=2, 4, 6, 8) far separated frequencies on the cutting accuracy for diverse beam numbers is calculated. The holistic combination effect becomes worse when more wavelengths are involved. The deteriorating trends of N-wavelength M-channel combination effects show great similarities. As the cutting residual increases, the combination effect first declines gently, then sharply decreases around the coherent length, and finally stabilizes at certain levels. Generally, the combination effect of a large array is worse than that of a small array. Accordingly, to gain a desirable combination effect with several wavelengths involved, especially for large beam number arrays, the variance of the chain length should be adjusted to be smaller than the coherent length.

References

[1] Augst S J, Fan T Y and Sanchez A 2004 *Opt. Lett.* **29** 474

[2] Fan T Y 2005 *IEEE J. Sel. Top. Quantum Electron.* **11** 567

[3] Xue Y H, He B, Zhou J, Li Z, Fan Y Y, Qi Y F, Yuan Z J, Zhang H B and Lou Q H 2011 *Chin. Phys. Lett.* **5** 054212

[4] He B, Lou Q H, Zhou J, Zheng Y H, Xue D, Dong J X,Wei Y R, Zhang F P, Qi Y F, Zhu J Q, Li J Y, Li S Y and Wang Z J 2007 *Chin. Opt. Lett.* **5** 412

[5] He B, Lou Q H, Zhou J, Dong J X, Wei Y R, Xue D, Qi Y F, Su Z P, Li L B and Zhang F P 2006 *Opt. Express* **14** 2721

[6] Fu S Y, Tian Z S, Shi X L and Sun Z H 2008 *Chin. Phys.* B **2** 0628

[7] Jia X J, Liu F N, Fu S G, Liu Y G, Yuan S Z and Dong X Y 2008 *Chin. Phys.* B **10** 2993

[8] Hecht E 2005 *Optics* (4th Edn.) (Beijing: Higher Education Press) p. 122

[9] Limpert J, Roser F, Klingebiel S, Schreiber T, Wirth C, Peschel T, Eberhardt R and Tiinnermann A 2007 *IEEE J. Sel. Top. Quantum Electron.* **13** 537

[10] Dajani I, Zeringue C, Bronder T J, Shay T, Gavrielides A and Robin C 2008 *Opt. Express* **16** 14233

[11] Dawson J W, Messerly M J, Beach R J, Shverdin M Y, Stappaerts E A, Sridharan A K, Pax P H, Heebner J E, Siders C W and Barty C P J 2008 *Opt. Express* **16** 1324

[12] Zhou P, Ma Y X, Wang X L, Ma H T, Xu X J and Liu Z J 2009 *Opt. Lett.* **34** 2939

[13] Wang X L, Zhou P, Ma Y X, Ma H T, Xu X J, Liu Z J and Zhao Y J 2010 *Chin. Phys.* B **19** 094202

[14] Wang X L, Zhou P, Ma Y X, Ma H T, Xu X J, Liu Z J and Zhao Y J 2010 *Chin. Phys. Lett.* **27** 124201

[15] Wang X L, Zhou P, Ma Y X, Ma H T, Xu X J, Liu Z J and Zhao Y J 2010 *Journal of Optics* **12** 75701

[16] Wang X L, Zhou P, Ma Y X, Ma H T, Xu X J, Liu Z J and Zhao Y J 2010 *Acta Phys. Sin.* **59** 5474 (in Chinese)

[17] Han K, Xu X J, Zhou P, Ma Y X, Wang X L and Liu Z J 2011 *Acta Phys. Sin.* **60** 074206 (in Chinese)

[18] Carhart G W, Ricklin J C, Sivokon V P and Vorontsov M A 1997 *Proc. SPIE* **3126** 221

[19] Vorontsov M A and Sivokon V P 1998 *J. Opt. Soc. Am.* A **15** 2745

[20] Zhou P, Liu Z J, Xu X J and Chen Z L 2008 *Appl. Opt.* **47** 3350

[21] Zhou P, Liu Z J, Xu X J, Chen Z L and Wang X L 2009 *Opt. Laser Technol.* **41** 268

[22] Stickley C M 2007 http://www.darpa.mil/mto/programs/adhels/index.htm

[23] Burnett J G and Jones J D C 1992 *Appl. Opt.* **31** 2977